

Strong-field photoionization of vibrational ground-state H_2^+ and D_2^+ molecules

C. Trump, H. Rottke, and W. Sandner

Max-Born-Institut, Rudower Chaussee 6, D-12489 Berlin, Germany

(Received 8 March 1999; revised manuscript received 17 June 1999)

We report on the observation of a high-energy ‘‘shoulder’’ in the kinetic-energy distribution of H^+ and D^+ ions formed in the interaction of H_2 and D_2 with ultrashort light pulses of an intensity higher than approximately 10^{15} W/cm². It extends up to a kinetic energy of ≈ 8 eV. The ‘‘shoulder’’ ions are formed by Coulomb explosion after photoionization of the respective molecular ion. The shape of the ‘‘shoulder’’ indicates that photoionization of H_2^+ in the vibrational ground state $v=0$ and of D_2^+ in $v=0,1$ is the mechanism for atomic ion formation near the ‘‘shoulder’’ cutoff. [S1050-2947(99)06111-9]

PACS number(s): 33.80.Rv, 33.80.Wz

I. INTRODUCTION

Molecular decay mechanisms in high-intensity ultrashort light pulses have been the subject of intense investigations. Special emphasis was always put on molecular hydrogen since already on this simplest molecule all mechanisms, specific at least to diatomic molecules, can be investigated and, what is of particular importance, even partly compared to theoretical results on molecular dynamics heavily perturbed by light. Most prominent contributions to molecular dissociation have been identified as bond-softening dissociation or above threshold dissociation (ATD) [1–5] (and Refs. cited there) and Coulomb explosion after stripping of more than one electron [6–9]. In the case of hydrogen all experimental data show that complete ionization is a stepwise process. First, one electron is photoionized with the nuclei at the H_2 equilibrium internuclear separation. The second electron is preferentially removed through charge resonance enhanced ionization (CREI) of H_2^+ after the internuclear separation has widened into a range between approximately 6 a.u. and 10 a.u. [6,9]. In all other diatomic molecules the removal of more than one electron with subsequent Coulomb explosion follows a similar pathway [7,8,10,11].

Here we investigate dissociative photoionization of hydrogen with the formation of charged dissociation products having a kinetic energy higher than that of Coulomb exploding ions formed via the CREI mechanism. These ions can be expected to give insight into the strong field properties of H_2^+ at small internuclear separations, a population of low lying H_2^+ vibrational states through the primary H_2 photoionization step, or possible nonsequential double ionization of H_2 at the equilibrium internuclear separation ($R_0 = 1.4$ a.u. [12]). In order to get information on how nuclear dynamics affects the formation of high energy dissociation fragments, we compare data for hydrogen and the isotope deuterium.

II. EXPERIMENT

We used pulses of a Kerr-lens mode locked Ti:sapphire laser at 790 nm amplified to a pulse energy of up to 2 mJ at 10 Hz repetition rate [13]. The pulse shape can be approximated by a Lorentzian intensity distribution with a full width at half maximum of ≈ 80 fsec. The linearly polarized laser

beam was focused to a focal spot diameter of ≈ 25 μm within the interaction region with the hydrogen and deuterium molecules. The light intensity was adjusted by a combination of a $\lambda/2$ -wave plate and a polarizer. Absolute values of the light pulse intensity based on the measured focal spot size, the pulse width, and the pulse energy are correct to within a factor of ≈ 2 . Despite this poor knowledge of absolute values relative to each other, intensities are correct to within $\pm 15\%$ of the respective value.

Hydrogen and deuterium were supplied in a well collimated pulsed supersonic beam. The H_2 gas purity was 99.999% and the D_2 purity 99.7% with H_2 as the main residual impurity. The velocity spread along the beam axis is estimated to be less than ± 60 m/sec for H_2 and ± 45 m/sec for D_2 . Transverse to the beam axis, the velocity spread is fixed by beam collimation to less than ± 5 m/sec (H_2) and ± 4 m/sec (D_2). This setup eliminates the thermal velocity spread present in a bulk gas sample which we found mainly limits the resolution achievable in measuring the kinetic energy of dissociation products [14].

An electric field free time-of-flight technique was used to determine the kinetic energy of fragment photoions emitted into a solid angle $\Omega = 5 \times 10^{-3}$ along the molecular beam axis. The polarization axis of the light beam coincided with this axis in the experimental runs. The solid angle subtended by the detector was practically independent of the kinetic energy of the ions in the energy range of interest here ($E_{\text{kin}} \geq 3$ eV). At the end of the drift tube we detected the ions with a microsphere plate (MSP). Single ion arrival times were measured with a time to digital converter with 1 nsec time resolution. The kinetic energy resolution achievable was limited by the geometry of the spectrometer setup to $\Delta E/E_{\text{kin}} = 0.05$ in an energy range $E_{\text{kin}} \leq 10$ eV.

Space charge in the focal spot of the laser beam did not affect the ion kinetic energy distributions. This was achieved by reducing the density in the molecular beam by a large separation between the nozzle and the focal spot (≈ 2 m). In the experimental runs we detected at most two H^+/D^+ ions in the solid angle subtended by the ion detector ($\Omega = 5 \times 10^{-3}$). Based on H^+ angular distributions measured in Ref. [15], a total emission solid angle of charged dissociation products of $\Omega \approx 0.9$ is determined. With these solid angles one calculates that no more than 1000 H^+/D^+ ions have been

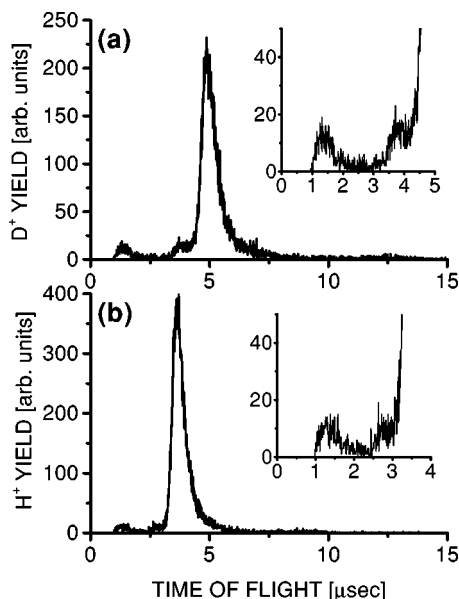


FIG. 1. Primary D^+ (a) and H^+ (b) time-of-flight spectra taken at a light intensity of $2.5 \times 10^{15} \text{ W/cm}^2$. The insets show on an enlarged scale the new plateaulike structures observed directly left of the rising edge at short flight times of the prominent lines in the spectra.

formed in the focal spot in each laser pulse if one assumes a detector efficiency of 50%. For a conservative estimate of the maximum kinetic energy gain of an H^+/D^+ ion due to the space charge of these ions, we assume that they are formed within a sphere with a diameter equal to the focal spot diameter of $25 \mu\text{m}$. This gives rise to a potential energy of less than 150 meV for an H^+/D^+ ion at the surface of this charge cloud. Thus 150 meV is an upper limit for the kinetic energy gain of the ions due to acceleration by the electric field of the space charge. As an independent check of space charge effects, we varied the backing pressure of the pulsed nozzle. No observable effect on the ion kinetic energy distributions was observed.

III. RESULTS AND DISCUSSION

In Fig. 1 we show primary ion time-of-flight (TOF) spectra for D^+ [Fig. 1(a)] and H^+ [Fig. 1(b)] which we measured at a light intensity of $2.5 \times 10^{15} \text{ W/cm}^2$ with 10 nsec time binning. No electric field was applied to accelerate the ions. The prominent feature in both spectra is Coulomb explosion after charge resonance enhanced photoionization (CREI) [6–8] of H_2^+ and D_2^+ , respectively. The corresponding lines appear at $4.9 \mu\text{sec}$ [D^+ , Fig. 1(a)] and $3.6 \mu\text{sec}$ [H^+ , Fig. 1(b)]. The plateaulike structures directly adjacent to the CREI lines at $3.7 \mu\text{sec}$ [D^+ , Fig. 1(a)] and $2.7 \mu\text{sec}$ [H^+ , Fig. 1(b)] are new features which will be relevant for the discussion below. They are shown on an expanded scale in the insets of the figure. For D_2^+ the new structure is more pronounced than for H_2^+ .

In the time-of-flight range below $\approx 2.5 \mu\text{sec}$ the ion signal observed in both spectra is completely formed by background gas photoionization. The spectra in Figs. 1(a) and 1(b) look very similar in this time interval. Since we did not apply electric fields for ion acceleration, the same back-

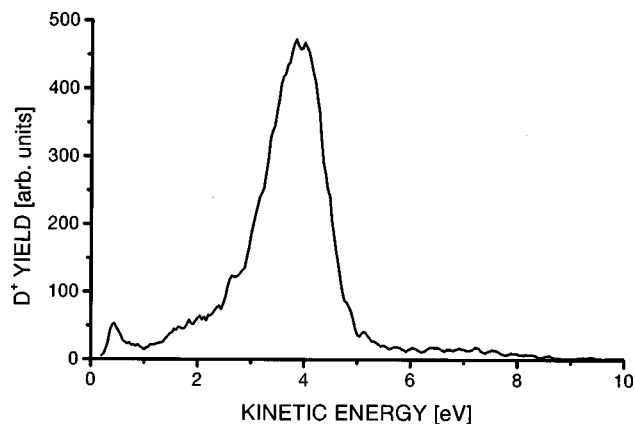


FIG. 2. D^+ ion kinetic-energy distribution at a light pulse intensity of $2.5 \times 10^{15} \text{ W/cm}^2$. Ions emitted along the polarization axis of the linearly polarized light wave are detected.

ground ions contribute to the yield in both time-of-flight spectra. These ions are extremely fast. Therefore we suspect that they are H^+ ions from either H_2O or residual hydrocarbon impurity dissociative photoionization. Since the experimental setup is not q/m , sensitive we cannot exclude the possibility that ions other than H^+ make up the background ion yield.

Figure 2 shows an overview kinetic energy distribution of D^+ ions formed by dissociative photoionization of D_2 at a light intensity of $2.5 \times 10^{15} \text{ W/cm}^2$. It was determined from the time-of-flight spectrum in Fig. 1(a) by a time to kinetic-energy transformation. The energy range extends from 0 up to 10 eV. Three main structures are observable. A quite narrow line near 0.5 eV ion kinetic energy, a broad hump with a steep high energy cutoff extending from about 1 eV to 5 eV, and a “shoulder” on a small signal level extending from $\approx 5.5 \text{ eV}$ up to $\approx 8 \text{ eV}$.

In a first step D_2 becomes photoionized in the high-intensity light pulse [16–20]. At the 790 nm excitation wavelength the 0.5 eV line in Fig. 2 is then formed by dissociation of D_2^+ after effective absorption of two laser photons ($\hbar\omega = 1.57 \text{ eV}$) [16–20]. Assuming unperturbed D_2^+ vibrational states, levels with vibrational quantum numbers $\nu=2,3,4$ contribute to photodissociation [21]. The broad hump with the maximum at a kinetic energy of approximately 4 eV has its origin in Coulomb explosion after photoionization of dissociating D_2^+ ions [17–21]. Charge resonance enhanced ionization (CREI) of D_2^+ at internuclear separations between $\approx 6 \text{ a.u.}$ and $\approx 10 \text{ a.u.}$ contributes to this structure [6–8] [17–21].

The high energy “shoulder” is the new structure which is most pronounced at high light intensity. It exists also for H_2 . To reveal its evolution with light intensity, Fig. 3 shows this part of the kinetic energy distributions for H_2 [Fig. 3(a)] and D_2 [Fig. 3(b)] on an enlarged scale. Corresponding spectra for H_2 and D_2 were recorded at equal light intensity [(1) $1 \times 10^{15} \text{ W/cm}^2$, (2) $1.5 \times 10^{15} \text{ W/cm}^2$, (3) $2.5 \times 10^{15} \text{ W/cm}^2$]. A “shoulder”-like structure is found at every intensity I . With decreasing I , the ion yield in the “shoulder” regime decreases. At the same time the lower bound E_{\min} of the kinetic-energy range where it is visible decreases. E_{\min} is determined by the position of the high

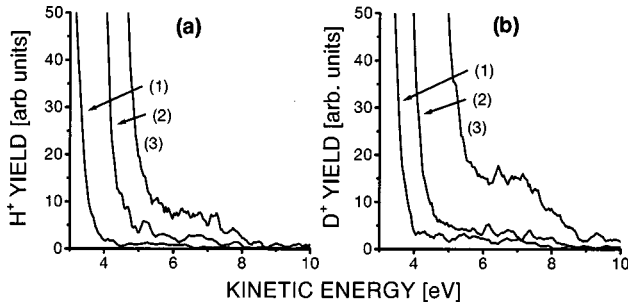


FIG. 3. High-energy part of (a) H^+ and (b) D^+ ion kinetic-energy distributions plotted on an expanded ion yield scale. Corresponding spectra were taken at equal light intensity: (1) $1 \times 10^{15} \text{ W/cm}^2$, (2) $1.5 \times 10^{15} \text{ W/cm}^2$, (3) $2.5 \times 10^{15} \text{ W/cm}^2$. The spectra reveal a “shoulder”-like structure at high kinetic energies.

energy cutoff of the CREI ion yield maximum (see Fig. 2). The high energy termination E_{max} of the “shoulder” is at $\approx 8 \text{ eV}$, nearly independent of the light intensity and isotopomere. Beyond E_{max} ($E_{\text{kin}} > 8.5 \text{ eV}$) the residual ion yield observable originates completely from decay of background gas molecules (see the TOF spectra in Fig. 1). The ratio of the mean ion yield in the “shoulder” to the maximum ion yield on the CREI structure increases with increasing light pulse intensity from 0.5% over 0.6% to 1% for H_2 [Fig. 3(a)] and from 0.8% over 1% to 3% for D_2 [Fig. 3(b)].

Similar to the interpretation of the CREI structure, we suspect Coulomb explosion of hydrogen and deuterium to be responsible for the ion yield in the “shoulder” region. In the case of H_2 and D_2 , the complete loss of electrons initiates Coulomb explosion. From the kinetic energy E_{kin} of a dissociation product (H^+ or D^+), the internuclear separation R at the instant of complete photoionization can be determined from

$$R = \frac{e^2}{2E_{\text{kin}} - E_0}. \quad (1)$$

Here e is the elementary charge and E_0 the kinetic energy of nuclear motion prior to complete photoionization. In the analysis of the data, E_0 will now be assumed to be small in comparison to $2E_{\text{kin}}$ in the “shoulder” region ($8 \text{ eV} < 2E_{\text{kin}} < 17 \text{ eV}$). This seems to be justified in view of dissociation product kinetic energies found in bond-softening and ATD at the excitation wavelength used here [16–21]. With E_0 set to zero it is possible to convert the ion kinetic energy distributions in Fig. 3 into ion yield distributions which are a measure of the probability of complete ionization of H_2 and D_2 as a function of internuclear separation (see, for example, [17]). They are shown in Fig. 4 for the “shoulder” ions.

Based on the transformation with $E_0 = 0$, the “shoulder” ions are formed by complete photoionization of the molecules at internuclear separations between 1.5 a.u. and 4 a.u. (Fig. 4). For both H_2 and D_2 , the R dependences of the ion yield in the “shoulder” develop a maximum at $R \approx 2 \text{ a.u.}$ at the highest light intensity. At lower intensities only a shoulder is formed similar to that in the kinetic-energy distributions. This is best visible in the D_2 results [Fig. 4(b)]. Inde-

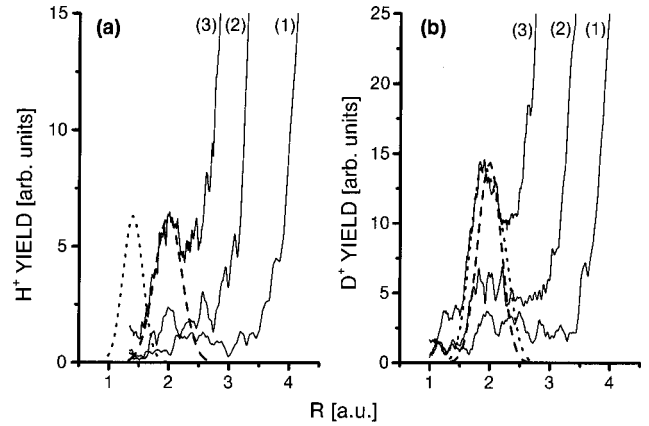


FIG. 4. Ion yield as a function of the internuclear separation R determined from the ion kinetic energy distributions (Fig. 3). Coulomb explosion of (a) H_2^+ and (b) D_2^+ with zero initial kinetic energy is the basis for the energy to R transformation. (a) Dashed line: $|\chi_0(R)|^2$ for the H_2^+ vibrational ground state, dotted line: $|\chi_0(R)|^2$ for the H_2 vibrational ground state. (b) Dashed line: $|\chi_0(R)|^2$ for the D_2^+ vibrational ground state, dotted line: $|\chi_0(R)|^2 + b|\chi_1(R)|^2 + c\chi_0(R)\chi_1(R)$. For the light intensities see Fig. 3

pendent of the light intensity, a small R cutoff in the ion yield is found at a nearly fixed internuclear separation. Charge resonance enhanced ionization (CREI) is impossible in the R range where the “shoulder” photoions are created. The necessary localization of the H_2^+ (D_2^+) electron is only possible at internuclear separations larger than approximately 6 a.u.

The maximum in the ion yield at $R = 2 \text{ a.u.}$ develops in a light intensity range between $1.5 \times 10^{15} \text{ W/cm}^2$ and $2.5 \times 10^{15} \text{ W/cm}^2$. It appears exactly at the equilibrium internuclear separation of H_2^+ and D_2^+ in the electronic ground state $1s\sigma_g$. This suggests that population in the $v = 0$ vibrational state is its origin. For a more detailed test of this assumption, we determined the nuclear wave function $\chi_0(R)$ of the unperturbed H_2^+ and D_2^+ vibrational ground states in the harmonic approximation. The vibrational frequency and equilibrium internuclear separations were taken from Ref. [12]. The probability distributions $|\chi_0(R)|^2$ to find H_2^+ and D_2^+ at an internuclear separation R are plotted as dashed lines in Fig. 4.

In the case of H_2^+ , $|\chi_0(R)|^2$ fits well to the experimentally observed ion yield maximum at $R = 2 \text{ a.u.}$ Especially its small R rising edge which is least influenced by the strong CREI yield maximum is well reproduced. This finding strongly supports the assumption that the $R = 2 \text{ a.u.}$ yield maximum is formed by photoionization of H_2^+ molecules in the vibrational ground state. Since we started from H_2 , this result gives further evidence that in general complete photoionization of hydrogen is a sequential process where first one electron is removed to yield H_2^+ . Direct double ionization of H_2 would give rise to an ion kinetic energy distribution which should resemble the H_2 vibrational ground-state wave function in the electronic state $X^1\Sigma_g^+$. The corresponding probability distribution is included in Fig. 4(a) as dotted line centered at $R = 1.4 \text{ a.u.}$ In this R range the ion yield is practically zero.

For D_2^+ [Fig. 4(b)] the probability distribution corresponding to the $v=0$ ground vibrational level is too narrow to reproduce the observed $R=2$ a.u. ion yield maximum. In order to get a better agreement at the low R rising edge of the yield maximum where the influence of the CREI peak is smallest, a possible way is to assume a population in the first excited vibrational state ($v=1$) of D_2^+ which also becomes photoionized. We took a possible population in this state into account in a partially coherent way and tried to reproduce the measured R dependence by a probability distribution of the form $a[\chi_0^2(R)+b\chi_1^2(R)+c\chi_1(R)\chi_2(R)]$ with χ_1 and χ_2 real valued nuclear wave functions. Similar to $v=0$, $\chi_1(R)$ was used in the harmonic approximation of the D_2^+ $1s\sigma_g$ potential-energy curve with the same equilibrium internuclear separation as for $\chi_0(R)$. A good fit is obtained for relative contributions $b=0.45$ and $c=-0.14$. The corresponding probability distribution is plotted in Fig. 4(b) as a dotted line. A pure incoherent superposition of χ_1 and χ_2 ($c=0$) would overestimate the observed ion yield for $R>2$ a.u. A pure coherent superposition would require $c=\pm 2\sqrt{b}$, that is $c=\pm 1.34$. The determined $c=-0.14$ therefore means that a nearly incoherent superposition of vibrational wave functions gives a good fit to the observed ion yield distribution.

For the given interpretation of the $R=2$ a.u. yield maximum to be justified, three conditions have to be fulfilled. First, the mean kinetic energy in the nuclear motion prior to removal of the second electron has to be small. This justifies the transformation from the ion kinetic-energy distribution to the R distribution using $E_0=0$ in Eq. (1). Since obviously only vibrational states $v=0,1$ are involved in formation of the maximum, this choice is reasonable. For these states $E_0<150$ meV, which is small compared to twice the kinetic energy of the ‘‘shoulder’’ ions.

Second, the ionization probability of the molecular ions has to be close to unity over the range of internuclear separations where the $v=0,1$ wave functions are different from zero. Only in this case can it be expected that the square of the wave function directly fits to the measured R dependence of the ion yield. To have an estimate of the necessary light intensity to meet this condition, we used the ADK (Ammosov, Delone, Krainov) expression [22] to approximate the ionization rate of H_2^+ for internuclear separations between 1 a.u. and 3 a.u. We calculated the probability for vertical ionizing transitions from the R -dependent ionization potential $I_p(R)$ [see Fig. 5(a)]. The results for several intensities between 8×10^{14} W/cm² and 2×10^{15} W/cm² are shown in Fig. 5(b). They are based on a light pulse of constant intensity I over a pulse duration of 80 fsec. This estimate shows that light pulse intensities approximately higher than 1.5×10^{15} W/cm² are necessary for nearly unity ionization probability over the relevant range of internuclear separations. The experimental intensity of appearance of the $R=2$ a.u. ion yield maximum is higher than this estimated necessary lower limit. This supports our interpretation of its origin.

Third, non-negligible population has to survive in the vibrational states $v=0,1$ up to light intensities $I>10^{15}$ W/cm². The experimental data indicate that for H_2^+ only $v=0$ remains populated while for D_2^+ at least a certain

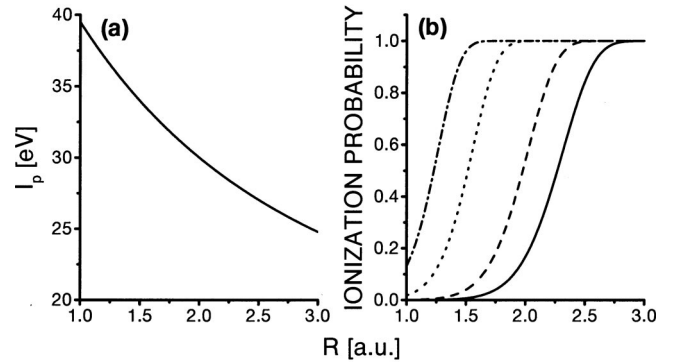


FIG. 5. (a) Dependence of the H_2^+ ionization potential on the internuclear separation R [24]. (b) The perpendicular ionization probability of H_2^+ as a function of internuclear separation R calculated for a flat top 80 fsec light pulse. Solid line: 8×10^{14} W/cm², dashed line: 1×10^{15} W/cm², dotted line: 1.5×10^{15} W/cm², dash-dotted line: 2×10^{15} W/cm².

population has to remain in $v=1$ to explain the details of the $R=2$ a.u. yield maximum in Fig. 4(b). Photodissociation is the population loss channel of these states. Via dissociation the internuclear separation increases into a regime where CREI nearly instantaneously serves to photoionize the molecular ion at the intensities used in the experiment [20]. Survival of population in $v=1$ for D_2^+ in contrast to H_2^+ under otherwise the same conditions may be explained in terms of the tighter binding of this vibrational state in case of D_2^+ and a lower velocity of nuclear motion. Depending on the internuclear separation R , dissociation can be initiated by the absorption of five to eleven laser photons between 1.5 a.u. and 2.5 a.u. This is the minimum number of photons necessary to excite the ions vertically to the lowest-lying repulsive excited electronic state $2p\sigma_u$. In the same R range, 18 to 22 photons are necessary for photoionization if one neglects the quiver energy of the free photoelectron. Comparing these numbers, it may be justified to assume that at the light intensity where efficient excitation to the dissociation continuum becomes possible, the inverse of the rate for absorption of further photons up to the ionization continuum is already smaller than the time it takes for the molecular ions to increase their internuclear separation significantly. Under these circumstances it becomes possible to map the ionic vibrational ground-state wave functions through Coulomb explosion as it is observed in this experiment. The higher yield of ‘‘shoulder’’ ions for D_2 compared to H_2 is probably a consequence of smaller nuclear velocities at comparable total energy deposited in the nuclear motion. It is certainly not an image of population differences created in the $v=0,1$ vibrational states by the primary H_2 and D_2 photoionization step since at least for unperturbed vibrational states of the ions the ionization Franck-Condon factors into the $v=0,1$ states are higher for H_2^+ [23].

Taking unperturbed stationary nuclear wave functions is the ‘‘simple man’s way’’ to model the maxima in the R dependence of the ion yield at $R=2$ a.u. At the light intensities used this is expected to be only a first approximation since the $1s\sigma_g$ electronic potential is distorted even at the relevant small internuclear separations. Additionally a dynamical evolution of population in the lowest vibrational lev-

els should be taken into account in a thorough theoretical analysis.

In conclusion, our experimental data give a hint at the population of low vibrational states of H_2^+ (D_2^+) by strong field ionization of the respective neutral molecule. But what is more surprising, a non-negligible amount of population remains there up to light intensities higher than 10^{15} W/cm^2 in pulses with a pulse width of ≈ 80 fsec. The results also show that complete photoionization even at these intensities is a strictly sequential process. No ions have been found

which correspond to complete photoionization at the equilibrium internuclear separation of H_2 or D_2 which may give a hint to nonsequential photoionization.

ACKNOWLEDGMENTS

We are grateful to Dr. M. Kalashnikov and G. Sommerer for their assistance in running the laser system used in this experiment.

-
- [1] A. Zavriyev, P. H. Bucksbaum, H. G. Muller, and D. W. Schumacher, *Phys. Rev. A* **42**, 5500 (1990).
- [2] B. Yang *et al.*, *Phys. Rev. A* **44**, R1458 (1991).
- [3] A. I. Pedarkov and L. P. Rapoport, *Opt. Spectrosc.* **65**, 55 (1988).
- [4] A. Giusti-Suzor, X. He, O. Atabek, and F. H. Mies, *Phys. Rev. Lett.* **64**, 515 (1990).
- [5] A. Giusti-Suzor *et al.*, *J. Phys. B* **28**, 309 (1995).
- [6] T. Zuo and A. D. Bandrauk, *Phys. Rev. A* **52**, R2511 (1995).
- [7] J. H. Posthumus, L. J. Frasinski, A. J. Giles, and K. Codling, *J. Phys. B* **28**, L349 (1995).
- [8] T. Seideman, M. Y. Ivanov, and P. B. Corkum, *Phys. Rev. Lett.* **75**, 2819 (1995).
- [9] S. Chelkowski, T. Zuo, O. Atabek, and A. D. Bandrauk, *Phys. Rev. A* **52**, 2977 (1995).
- [10] S. Chelkowski and A. D. Bandrauk, *J. Phys. B* **28**, L723 (1995).
- [11] M. Ivanov *et al.*, *Phys. Rev. A* **54**, 1541 (1996).
- [12] K. P. Huber and G. Herzberg, *Molecular Spectra and Molecular Structure, IV. Constants of Diatomic Molecules* (Van Nostrand Reinhold Company, New York, 1979).
- [13] M. P. Kalashnikov, G. Sommerer, P. V. Nickles, and W. Sandner, *Quantum Electron.* **27**, 403 (1997).
- [14] J. Ludwig, H. Rottke, and W. Sandner, *Phys. Rev. A* **56**, 2168 (1997).
- [15] J. H. Posthumus *et al.*, *J. Phys. B* **31**, L553 (1998).
- [16] A. Zavriyev, P. H. Bucksbaum, J. Squier, and F. Saline, *Phys. Rev. Lett.* **70**, 1077 (1993).
- [17] G. N. Gibson, M. Li, C. Guo, and J. Neira, *Phys. Rev. Lett.* **79**, 2022 (1997).
- [18] T. D. G. Walsh, F. A. Ilkov, and S. L. Chin, *J. Phys. B* **30**, 2167 (1997).
- [19] M. R. Thompson *et al.*, *J. Phys. B* **30**, 5755 (1997).
- [20] T. D. G. Walsh *et al.*, *Phys. Rev. A* **58**, 3922 (1998).
- [21] C. Trump, H. Rottke, and W. Sandner, *Phys. Rev. A* **59**, 2858 (1999).
- [22] M. V. Ammosov, N. B. Delone, and V. P. Krainov, *Zh. Éksp. Teor. Fiz.* **91**, 2008 (1986) [*Sov. Phys. JETP* **64**, 1191 (1986)].
- [23] G. Dunn, *J. Chem. Phys.* **44**, 2592 (1966).
- [24] T. E. Sharp, *At. Data* **2**, 119 (1971).